Depth-map-based shape recognition of soft continuum manipulator body

Jan Fraś

Przemysłowy Instytut Automatyki i Pomiarów, PIAP
al.Jerozolimskie 202, 02-486 Warsaw, Poland
jfras@piap.pl

Abstract. Soft robotics is young and dynamically evolving field of scientific research. Soft robots are difficult to control and much more complex for modeling than traditional robots. They are, however, gaining more and more researchers' interest due to their high potential. Soft robot body is made of flexible materials and it contains no rigid or discrete joints, its movement is generated by smooth and continuous deformation of the body. The softness of the body enables wide range of possible robot configurations which, on the other hand, are difficult to measure or predict. There were many shape detection approaches proposed so far, but most of them provide only discrete manipulator points position. Such a solution is not sufficient for some applications, since the manipulator body configuration in between the measured points is uncertain. In this paper Authors propose algorithm for continuous detection of the flexible manipulator shape. The algorithm is based on depth image provided by sensor such as Kinect. The depth image is processed in steps: detection of the manipulator central axis, the axis 3D shape reconstruction and orientation approximation for each point that lies on it. Numerical representation of the manipulator surface is also generated. The data obtained can be used for manipulator internal state correction including its input values and external disturbances.

1 Introduction

Continuum manipulators are widely considered as a replacement for the traditional robots composed of a rigid parts. They are gaining more and more interest due to their safety properties and manipulation capabilities unachievable for the conventional machines. Continuum robots have no traditional prismatic or rotational joints and soft materials they are made of make them safe in contact with external objects. Smooth deformation of tehir body make them able to generate motion and shape unreachable for traditional robots. Such adwantages make soft robots for a variety of tasks that require enormous dexterity and softness like minimal invasive surgery, soft objects manipulation or tasks that require a human interaction [1,2,3,4].

Traditional manipulator deformation can be easily detected by encoders housed in joints. Joints configuration combined with well defined kinematics

makes rigid robot shape detection easy. Soft robot consists no rigid parts connected by any discrete joints, but any movement is generated by smooth deformation of their body. Because of that soft robot's kinematics is much more complex. Another issue is that any external force applied to the manipulator causes a distributed deformation, that can not be neither easily measured nor predicted or modeled. Moreover there are no relevant sensors available for proper shape detection. Many sensors were proposed but since soft robot can deform to very complex shapes the data they provide individually is not satisfying for effective shape reconstruction [5,6,7]. Due to above issues, soft robot configuration detection is a complex task and requires much more effort when comared to any traditional devices.

In this paper we propose a custom shape reconstruction method for a continuum manipulator of a cylindrical shape. The method is based on a depth image provided by a single Kinect sensor. The method does not require any expensive tracking systems or sensors and provide continuous configuration approximation. The method was developed for the Stiff-Flop [8] manipulator for modeling validation purposes.

The data obtained by the algorithm can be used for manipulator control loop closure, modeling validation purposes, learning and other soft robotics related purposes.

2 Manipulator description

The algorithm presented in this paper has been designed for a cylindrical continuum manipulator [8], Figure 1. The manipulator's body is assumed to be smooth and to have constant diameter value along its length.

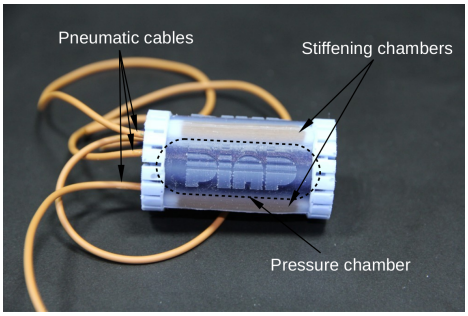

Fig. 1: Single module of Stiff-Flop manipulator

The configuration of such manipulator can be described in many different ways. Most popular methods are based on Constant Curvature approach. Such methods assume that the robot can be divided to a modules and each of the

module can be defined by a fragment of a circle using its length, curvature and curvature direction [9].

Constant curvature assumption is not always fulfilled and thus more complex methods has been proposed such as very general finite method elements analyzes or custom kinematics models based on physical principles [10,7].

In this paper we use 3D curve defined by a set of points to describe the manipulators backbone shape.

3 Algorithm

3.1 The depth image data

The Kinect senor used for this work provides a depth image. Depth image can be expressed as a gray-scale image with a distance information coded in each pixel value, Image 2a. 3D point position corresponding to each image pixel can be retrieved by using a set of two linear equations. Due to that the data can be processed in convenient image format and then converted into 3D space.

3.2 Algorithm steps

The subsequent steps of the algorithm has been presented in Figure 2b. Using depth gray-scale image, the manipulator is separated from the background using adaptive thresholding. As the manipulator base position is usually well defined it is used as the starting point for thresholding procedure. The segmentation result and source image is presented in Figure 3.

Using the segmented depth image a projection of the manipulator center-line on the image plane (ridge) is found. The ridge detection is made in two steps: an intersection of two paths starting form a random points (Figure 4a in the manipulator projection is chosen as an initial point on the ridge, Figure 4b. The paths are defined by a gradient-like procedure described below. When the initial point is found the ridge is propagated up and down along the manipulator's body, Figure 4c. The hinge propagation procedure is similar to the gradient-like procedure used for the initial point detection; the algorithm moves step by step in a direction indicated by the currently processed pixels spread on a circle around the current position (1). The processed pixel values are considered as a function of angle. There are two minima expected in such a function as the considered pixels are located on a cylindrical manipulator's shape, Figure 5. Since the depth data is discrete and noisy the direction determined by a minimum of (1) does not assure any reasonable results. Thus a continuum function (2) is fitted to the data and its extrema are used for further analysis.

$$f(\varphi) = \frac{p(x + rcos(\varphi), y + rsin(\varphi)) - p(x, y)}{r} \tag{1}$$

where $p(x, y)$ denotes the value of the pixel at x column and y row of the image, r stands for the radius of the circle the pixels are located on.

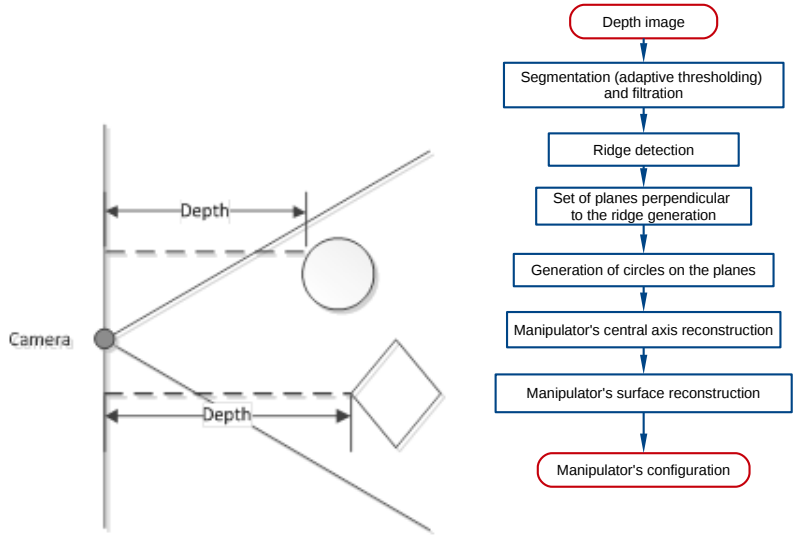

(a) (b)

Fig. 2: a) Kinect sensor data [11], b) algorithm flowchart

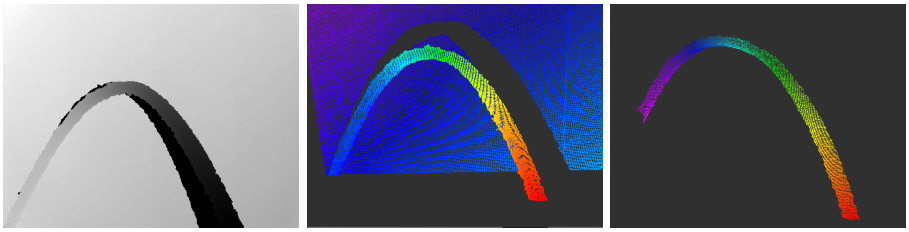

(a) (b) (c)

Fig. 3: a) gray-scale depth image, b) 3D point cloud, c) points after background filtration

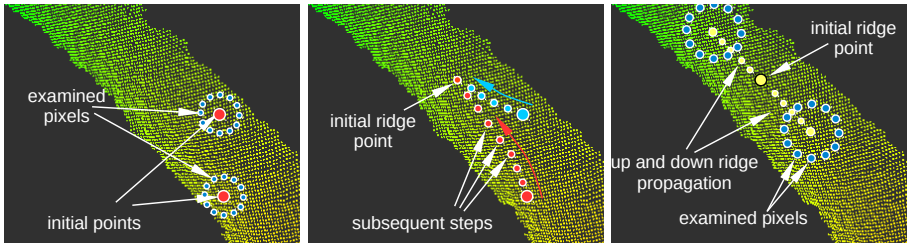

(a) (b) (c)

Fig. 4: Ridge detection procedure; a)random points as a starting positions, b)intersection of gradient-like paths as a starting point for the ridge, c) ridge propagation

$$f_1(\varphi) = a_1 cos(\varphi + a_2) + (a_3\varphi + a_4)cos(2\varphi + a_5) + a_6 \tag{2}$$

$$f_2(\varphi) = a_7 cos(\varphi + a_8) + a_9 \tag{3}$$

where $a_1, a_2 ... a_9$ stand for the optimized values.

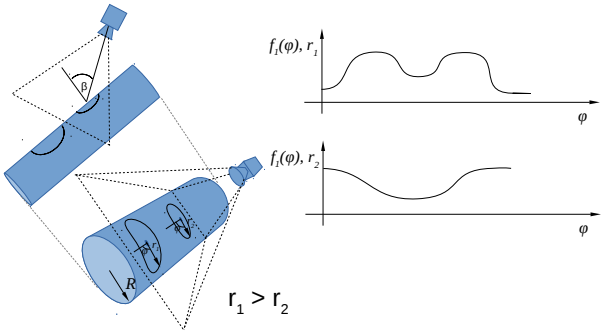

(a)

Fig. 5

The r value is crucial since too small r value may cause undesired function (1) shape, Figure 5. This is because the derivate of cylinder surface distance to the sensor plane around the considered point equals zero in the cylinder radial direction. The r value is chosen to assure both expected minima to be visible in the plot. As both minima are initially determined, the data is processed again for the φ variable limited to a small value around the minima. For those

values another function (3) is fitted in order to precisely calculate next iteration position. This limitation is necessary since the whole range fitting is vitiated by a significant error and the fitted extrema do not perfectly correspond with the data. The results of initial and final minima detection is presented in Figure 6.

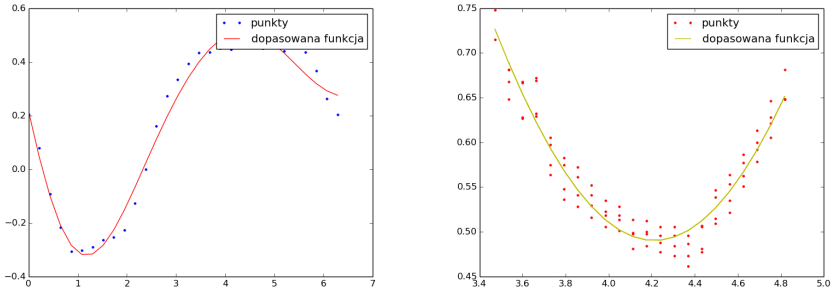

(a) (b)

Fig. 6: Minimas detection precision visible: a) preliminary detection for the whole circle, b) precise minimum determination for a limited angle, much more data taken into account

Using the path propagated along the manipulator's image the 3D ridge shape is computed. Once that is done, the 3D manipulator surface is splited by a set of planes. Each plane corresponds with a point of the ridge and is perpendicular to the ridge at that point. All the points from the manipulator's surface being closer to the plain than a threshold value are marked for further computing that is circles fitting. Each fitted circle corresponds with a manipulator cross-section contour. After the contours are defined their centers are filtered and connected to compose the manipulator's central axis. As the central axis is known, the manipulator's surface is reconstructed. The subsequent stages are presented in Figure 7.

4 Conclusion

At the moment the publication was written, the algorithm validation against a real manipulator was not yet performed due to the material properties of the available manipulator. The manipulator was made of a transparent silicone that is not properly detected by the Kinect sensor.

Using the presented approach we managed to reconstruct the shape of a cylindrical curved object with 40mm of diameter, however, the algorithm is not stable and its performance depends on the initial point choice, the object shape, dimension and its distance from the sensor. The data provided by the sensor is noisy and the depth resolution is low. Moreover the noise is not easy to filter as

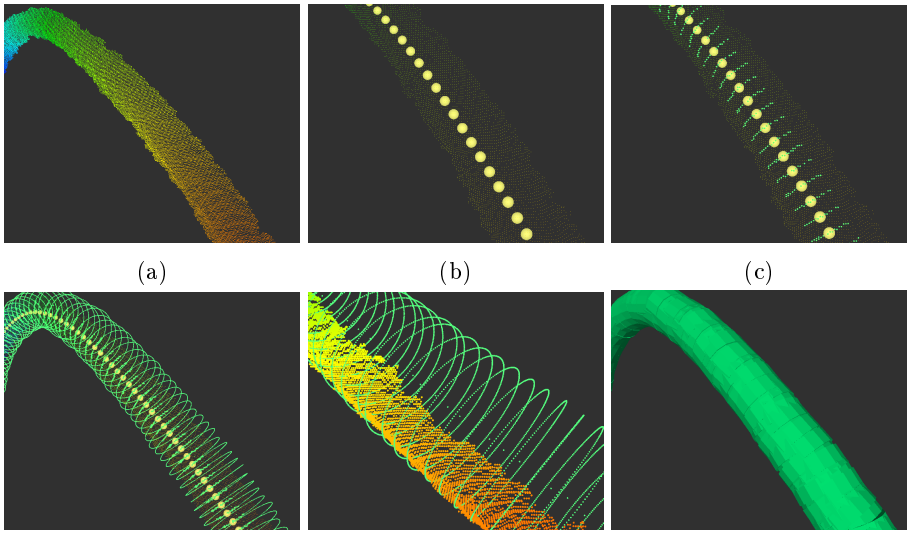

Fig. 7: Subsequent stages: a) raw data points, b) ridge detected (yellow dots), c) data classification for circles fitting (green points) d), e) fitted circles, f) fitted surface

its distribution depends on the pixel position and is related to the pattern the sensor projects on the object. Due to the poor data quality the algorithm often fails.

Another issue is that the algorithm does not behave in a stable way at the edges of the object where the data is not complete and even more noisy. The backbone in these areas is often not properly reconstructed. In the presented work we also assumed lack of any discontinuities, that is usually not fulfilled, as most of the manipulators have some connections between the continuum parts that would probably introduce some additional errors.

The proposed algorithm shows a potential to properly reconstruct the shape of curved cylindrical objects, however, it can not be used for manipulator's shape reconstruction due to low stability and very high noise to signal ratio.

References

1. Carmel Majidi. Soft robotics: a perspective—current trends and prospects for the future. *Soft Robotics*, 1(1):5–11, 2014.
2. Ellen T Roche, Markus A. Horvath, Ali A. Nodeh, Kevin C. Galloway, Nikolay V. Vasilyev, David J Mooney, Frank A Pigula, and Conor J Walsh. Design And Fabrication Of A Soft Robotic Direct Cardiac Compression Device. In *Proceedings of the ASME 2015 International Design Engineering Technical Conferences & Computers and Information in Engineering Conference (IDETC/CIE 2015)*, Boston, MA, 2-5 Aug 2015 2015.

3. Bobak Mosadegh, Panagiotis Polygerinos, Christoph Keplinger, Sophia Wennstedt, Robert F. Shepherd, Unmukt Gupta, Jongmin Shim, Katia Bertoldi, Conor J. Walsh, and George M. Whitesides. Pneumatic Networks for Soft Robotics that Actuate Rapidly. *Advanced Functional Materials*, 24(15):2163–2170, 2014.
4. Alberto Arezzo, Yoav Mintz, Marco Ettore Allaix, Simone Arolfo, Marco Bonino, Giada Gerboni, Margherita Brancadoro, Matteo Cianchetti, Arianna Menciassi, Helge Wurdemann, et al. Total mesorectal excision using a soft and flexible robotic arm: a feasibility study in cadaver models. *Surgical Endoscopy*, pages 1–10, 2016.
5. T. C. Searle, K. Althoefer, L. Seneviratne, and H. Liu. An optical curvature sensor for flexible manipulators. In *Robotics and Automation (ICRA), 2013 IEEE International Conference on*, pages 4415–4420, May 2013.
6. Y. Noh, S. Sareh, J. Back, H. A. Würdemann, T. Ranzani, E. L. Secco, A. Faragasso, H. Liu, and K. Althoefer. A three-axial body force sensor for flexible manipulators. In *2014 IEEE International Conference on Robotics and Automation (ICRA)*, pages 6388–6393, May 2014.
7. Jan Fraś, Jan Czarnowski, Mateusz Maciaś, and Jakub Główka. *Static Modeling of Multisection Soft Continuum Manipulator for Stiff-Flop Project*, pages 365–375. Springer International Publishing, Cham, 2014.
8. Jan Fras, Jan Czarnowski, Mateusz Macias, Jakub Główka, Matteo Cianchetti, and Arianna Menciassi. New STIFF-FLOP module construction idea for improved actuation and sensing. In *ICRA*, pages 2901–2906. IEEE, 2015.
9. Robert J Webster and Bryan A Jones. Design and kinematic modeling of constant curvature continuum robots: A review. *The International Journal of Robotics Research*, 2010.
10. Christian Duriez. Control of Elastic Soft Robots based on Real-Time Finite Element Method. In *ICRA 2013 IEEE International Conference on Robotics and Automation*, Karlsruhe, France, 2013.
11. Microsoft Kinect. https://dev.windows.com/en-us/kinect.